Full Paper
ELECTROANALYSIS

Minimally-invasive Microneedle-based Biosensor Array for Simultaneous Lactate and Glucose Monitoring in Artificial Interstitial Fluid

*Paolo Bollella[a], Sanjiv Sharma[b], Anthony Edward George Cass[c], Riccarda Antiochia[a,]**

[a] Department of Chemistry and Drug Technologies - Sapienza University of Rome, Rome, Italy

[b] College of Engineering - Swansea University, Swansea, Wales

[c] Department of Chemistry & Institute of Biomedical Engineering - Imperial College, London, UK

* e-mail: corresponding author: riccarda.antiochia@uniroma1.it

Abstract

Here we report the first mediated pain free microneedle-based biosensor array for the continuous and simultaneous monitoring of lactate and glucose in artificial interstitial fluid (ISF). The gold surface of the microneedles has been modified by electrodeposition of Au-multiwalled carbon nanotubes (MWCNTs) and successively by electropolymerization of the redox mediator, methylene blue (MB). Functionalization of the Au-MWCNTs/polyMB platform with the lactate oxidase (LOX) enzyme (working electrode 1) and with the FAD-Glucose dehydrogenase (FADGDH) enzyme (working electrode 2) enabled the continuous monitoring of lactate and glucose in the artificial ISF. The lactate biosensor exhibited a high sensitivity (797.4 ± 38.1 μA cm^{-2} mM^{-1}), a good linear range (10-100 μM) with a detection limit of 3 μM. The performances of the glucose biosensor were also good with a sensitivity of 405.2 ± 24.1 μA cm^{-2} mM^{-1}, a linear range between 0.05 and 5 mM and a detection limit of 7 μM. The biosensor array was tested to detect the amount of lactate generated after 100 minutes of cycling exercise (12 mM) and of glucose after a normal meal for a healthy patient (10 mM). The results reveal that the new microneedles-based biosensor array seems to be a promising tool for the development of real-time wearable devices with a variety of sport medicine and clinical care applications.

Keywords: Microneedles; Lactate; Glucose; Simultaneous monitoring; Artificial interstitial fluid; Minimally invasive sensor.

1 Introduction

Microneedles were initially utilized in 1976 by Gestel and Place for transdermal drug delivery [1-3]. More recently, there has been an increased focus on the use of microneedles for the development of diagnostic sensors by accessing the interstitial fluid (ISF) [4]. In the last decade, many efforts have

been focused to achieve the clinical translation of microdevices for the continuous on-body monitoring of relevant bioanalytes (e.g. glucose, lactate, glutamate, etc.) [5-8]. On this purpose, microneedle arrays have gained considerable interest within the biomedical community due to the promise of pain-free biosensing and highly integrated biocompatible devices, which can be easily fabricated on industrial scale and at low costs [9-12]. The rapid development of transdermal drug delivery and minimally invasive analytical devices led to manufacture microneedles of different geometries, designs and materials (including polymers, metals, glass, carbohydrates or silicon). Other applications of microneedle technology have also been investigated including biopsy [13-14], light delivery to deeper skin layers for diagnosis and treatment of epithelial cancers [15] and for measurement of electrical potentials (e.g. electrocardiography) [16-18].

Nowadays, considering the technological progress on microfabrication, microneedle array-based biosensors enable the monitoring of different bioanalytes in the dermal ISF [19-20], which is definitely a more accessible and more reproducible matrix compared to human blood, sweat, urine and saliva [21-22]. Most biomarkers monitored in the ISF microenvironment exhibit a good correlation with their venous blood levels [23-24]. Due to the shorter length of the microneedles (1 mm) compared for example to the commercially available needle sensors used for continuous glucose monitoring (CGM), they can penetrate the stratum corneum but they do not reach deep into the dermis (Fig. 1) [25-26]. According to medical knowledge, the upper part of the dermal interstitial compartment should contain neither blood vessels nor nerve endings. For these reasons the microneedle arrays offer the following advantages: i) they are minimally invasive, thanks to their small dimensions; ii) they show reduced biofouling effects, as they are changed on a daily basis (24-48 hours) compared to other implantable devices which are changed every 7-14 days; iii) they provide larger currents because of their larger surface areas [27]. Moreover, microneedle arrays prevent risk of skin irritation, local infection bleeding and reduce pain and tissue trauma. A full recovery is observed within 24 hours after removal [19].

Furthermore, skin ISF provides a wide range of vital information by using a continuous and non-invasive fashion. In the last 20 years, ISF was used also for non-invasive detection of inherited metabolic diseases, organ failure, and drug efficacy [12, 28]. Nevertheless, most of the attention has been devoted on glucose monitoring [29-31]. The good correlation between ISF and blood glucose concentration has prompted several researchers to develop optical-, ultrasound-, heat-, and electrochemical-based devices for continuous, non-invasive monitoring of other metabolites such as lactate and alcohol [32-33].

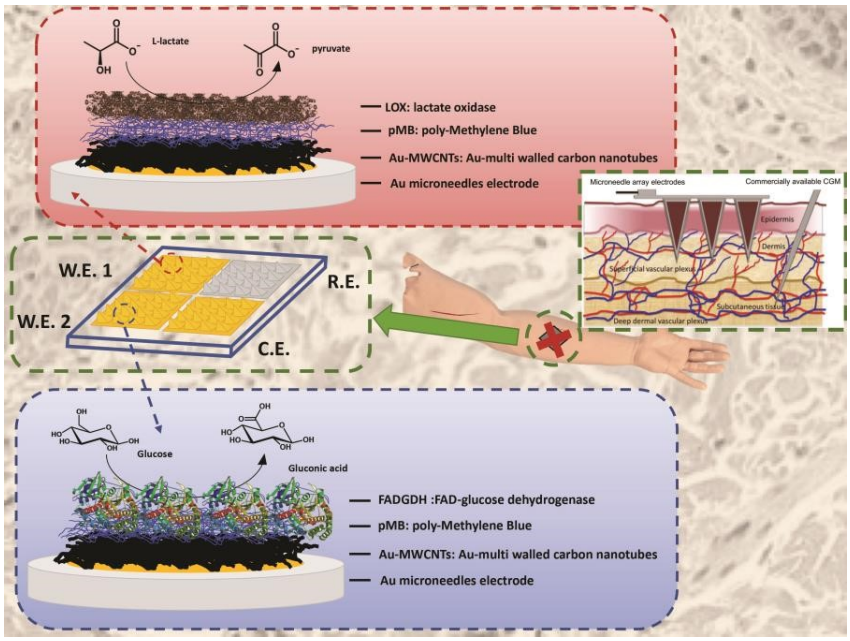

Fig.1. Schematic representation of microneedle-based biosensor array for simultaneous lactate and glucose monitoring in artificial interstitial fluid. W.E.1=working electrode 1; W.E.2=working electrode 2; R.E.= reference electrode; C.E.= counter electrode.

The present work describes the first example of a mediated pain free microneedle-based biosensor array for the simultaneous monitoring of lactate and glucose in the ISF. The microneedle array works as seconf generation biosensor thanks to the electrodeposition of Au-multiwalled carbon nanotubes (MWCNTs) onto the gold surface of the microneedles and to the electropolymerization of the mediator methylene blue (MB). The Au-MWCNTs/polyMB platform was successively functionalized with the LOX enzyme (W.E.1) and the FAD-Glucose dehydrogenase (FADGDH) enzyme (W.E.2) by a simple drop casting procedure to enable the continuous monitoring of lactate and glucose in artificial ISF, as schematized in Figure 1.

The device was also tested to monitor the amount of lactate and glucose generated after 100 minutes of cycling exercise and after a normal meal for a healthy patient, respectively. Both cases were studied simulating the substrate diffusion through a chitosan/agarose hydrogel skin model embedded in the

ISF, using a flow injection system. The promising analytical performances showed by the new microneedle-based biosensor array makes it an interesting tool as a pain free wearable device for continuous monitoring of lactate and glucose for sport and medical applications.

2. Experimental

2.1 Chemicals and Reagents

4-(2-Hydroxyethyl)piperazine-1-ethanesulfonic acid (HEPES), agarose, ammonium chloride (NH_4Cl), ascorbic acid (AA), boric acid, calcium chloride ($CaCl_2$), chitosan with medium molecular weight, D-(+)-glucose (Glc), magnesium sulfate ($MgSO_4$), methylene blue (MB), multi-walled carbon nanotubes (MWCNTs), potassium chloride (KCl), potassium nitrate (KNO_3), saccharose, sodium tetraborate, sodium chloride (NaCl) sodium L-lactate, sodium phosphate monobasic (NaH_2PO_4), sulfuric acid (H_2SO_4), tris(hydroxymethyl)aminomethane (TRIS) and uric acid (UA) were obtained from Sigma Aldrich (St. Louis, MO, USA).

Lactate oxidase (LOX) from *Aerococcus Viridans* was obtained from Creative Enzyme Ltd. The LOX (activity 106 U/ml) was dissolved in a phosphate buffer at pH 6.5and kept at -20 °C until immediately before being used [34].

FAD-Glucose dehydrogenase (FADGDH) from *Aspergillus niger* was obtained from Creative Enzyme Ltd. GDH (activity 300 U ml^{-1}) was dissolved in a phosphate buffer at pH 7, divided into aliquots, and kept at -20 °C until immediately before being used [35].

The artificial interstitial fluid (ISF) was prepared by mixing 2.5 mM $CaCl_2$, 5.5 mM glucose, 10mM Hepes, 3.5 mM KCl, 0.7 mM $MgSO_4$, 123 mM NaCl, 1.5 mM NaH_2PO_4, 7.4 mM saccharose. The pH was adjusted to pH 7 [36].

All solutions were prepared using Milli-Q water (18.2 MΩ cm, Millipore, Bedford, MA, USA).

2.2 Electrode Preparation and Modification

The microneedle array base structures were fabricated in polycarbonate at Glasgow University, as described in detail previously and metallised by Torr Scientific Ltd (Bexhill) [37]. They consist of a polycarbonate structure (1.0 × 1.0 x 0.2 cm) consisting of 64 microneedles perpendicular to the base plate arranged as four 4x4 arrays. The dimensions of the pyramid are the following: base 0.06 cm, height 0.1 cm; 4x4 array area: 0.2 cm^2. Three arrays have been metallized with gold and two of them

are used as working electrodes and one as counter electrode. The other array has been metallized with silver. However, in this work an external saturated calomel electrode was used as reference electrode. The working electrodes were modified according to a protocol developed in our group [20]. Briefly resuming, the microneedle-based electrodes were cleaned in 0.5 M H_2SO_4 by cycling 20 times between − 0.3 and 1.7 V vs. SCE at a scan rate of 300 mV s^{-1} and then were modified by electrodeposition of Au-MWCNTs by sweeping the potential between 0.8 and 0 V vs. SCE for 25 scans at 50 mV s^{-1} in a suspension containing 5 mg mL^{-1} of MWCNTs (10 mM $HAuCl_4$ in 2.5 M NH_4Cl) [38]. Afterwards, the Au microneedle/Au-MWCNTs electrodes were further modified by electropolymerization of MB by sweeping the potential between -0.4 and 1.2 vs. SCE in 0.25 mM MB solution (0.02 M borate buffer pH 9.14, supporting electrolyte 0.1 M KNO_3, sweep rate 50 mV s^{-1}) [39-41]. Next, 5 µL of LOX and 5 µL of FADGDH were drop-cast onto two different 4x4 arrays, for lactate and glucose biosensor respectively, and let them dry at room temperature.

2.5 Electrochemical Measurements

Cyclic voltammetry and amperometric experiments were performed by using a bipotentiostat (Dropsens-Metrohm, The Netherlands) controlled by Dropview 200 software (Dropsens-Metrohm, Eco Chemie, The Netherlands) with a conventional three-electrodes electrochemical cell equipped with two Au microneedles 4x4 arrays as working electrodes, a saturated calomel electrode (SCE, 244 mV vs. NHE, Cat. 303/SCG/6, AMEL, Milano, Italy) as reference electrode and a microneedle 4x4 array as counter electrode. The temperature-controlled experiments were carried out by using a thermostatic bath (T ± 0.01 °C, LAUDA RM6, Delran, NJ, USA).

2.6 Simultaneous Monitoring of Lactate and Glucose in Artificial ISF by Using an Agarose Hydrogel Skin Model

Amperometric experiments were performed by using a flow injection system equipped with a peristaltic pump (Gilson, Villier-le-Bel, France) to keep the flow rate at 30 mL min^{-1} and a six-port valve electrical injector (Rheodyne, Cotati, CA, USA). The chitosan/agarose hydrogel was prepared by dissolving 0.4 g of agarose in 0.5% (w/v) aqueous chitosan solution. Afterwards, the solution was poured in Teflon molds (~8 mm in diameter and ~5 mm in height) and maintained overnight at 4 °C to allow the mixtures to gel, according to protocols reported in literature [42]. Thereafter, the so prepared chitosan/agarose hydrogel was embedded in artificial ISF and placed into a Petri dish connected to the

flow injection system. Then, the microneedles-based biosensor array was placed onto the chitosan/agarose hydrogel measuring the amount of lactate produced after 100 minutes of cycling exercise (12 mM) and the glucose intake levels after meal for a healthy patient (10 mM) [43-44]. Both lactate and glucose concentrations were selected according to data reported in literature [45].

3. Results and Discussion

3.1 Electrochemical Characterization of Lactate Biosensor in Artificial ISF

Lactate biosensors were realized by immobilization of LOX enzyme by a simple drop-casting procedure on the Au microneedle/Au-MWCNTs/pMB electrode, previously modified as reported in section 2.2, according to a procedure developed and optimized in our group [20].

The electrochemical performances of the Au microneedle/Au-MWCNTs/pMB/LOX biosensor were evaluated by cyclic voltammograms (CVs) experiments performed both in non-turnover (artificial ISF) and turnover conditions (artificial ISF spiked with 10 mM sodium L-lactate). Au microneedle/Au-MWCNTs/pMB/LOX electrode exhibited a couple of quasi-reversible peaks ($E^{0'}$=-95 mV vs. SCE) due to pMB (Fig. 2A, black curve), while a great electrocatalysis starting at E_{ONSET}= -95 mV vs. SCE and rising up to 370 μA cm^{-2} at +0.5 vs. SCE is observed in the presence of 10 mM sodium L-lactate (Fig. 2A, red curve). Such low potential for lactate oxidation reflects the efficient electron donor-acceptor interactions between the carbon nanotubes and the pMB, which is able to shuttle the electrons between the redox center of LOX and the electrode surface [46-47].

The analytical response of the lactate biosensor was evaluated by chronoamperometry at a fixed applied potential (E_{app}= +0.15 V vs. SCE) in order to avoid any interferences, as reported in Figure 2B. The calibration curve for lactate detection in artificial ISF, shown in Figure 2C, indicates a linear range from 10 μM to 100 μM lactate, a detection limit of 3 μM (based on S/N=3) and a very high sensitivity (797.4 ± 38.1 μA cm^{-2} mM^{-1}) with a correlation coefficient of 0.96 (RSD 5.0 %, n=3). The calibration curve was also fitted to the classical Michaelis-Menten kinetic parameters, with a J_{max} of 298 ± 8 μA cm^{-2} and an apparent Michaelis-Menten constant (K_M) of 0.67 ± 0.1 mM [48].

3.2 Electrochemical Characterization of Glucose Biosensor in Artificial ISF

Similar to lactate biosensors, glucose biosensors were realized by immobilization of FADGDH enzyme by a simple drop-casting procedure on the Au microneedle/Au-MWCNTs/pMB electrode, previously modified according to a procedure developed and optimized in our group (section 2.2) [20].

The performances of the Au microneedle/Au-MWCNTs/pMB/FADGDH electrode have been first evaluated by using cyclic voltammetry and then chronoamperometry at a fixed potential. As for the lactate biosensor, in absence of the substrate a couple of quasi-reversible peaks due to the MB electropolymerized onto the modified electrode surface was observed for the Au microneedle/Au-MWCNTs/pMB/FADGDH electrode in artificial ISF (Fig. 3A, black curve). In presence of 10 mM glucose, an electrocatalytical wave starting at E_{ONSET}= -110 mV vs. SCE and rising up to 428 μA cm^{-2} at +0.5 vs. SCE, is clearly observed, as shown in Fig. 3A. The analytical response of the glucose biosensor was evaluated by chronoamperometry at a fixed applied potential (E_{app}= +0.15 V vs. SCE) (Fig. 3B). The calibration curve for glucose detection in artificial ISF, shown in Figure 3C, shows an extended linear range from 50 μM to 5 mM glucose, a detection limit of 7 μM (based on S/N=3) and a good sensitivity (405.2 ± 24.1 μA cm^{-2} mM^{-1}) with a correlation coefficient of 0.98 (RSD 6.7 %, n=3). Once again , a J_{max} of 719 ± 15 μA cm^{-2} and an apparent Michaelis-Menten constant (K_M) of 7.9 ± 0.4 mM were calculated by fitting the calibration curve to the classical Michaelis-Menten kinetic parameters [49].

Moreover, the cross-talking behaviour of the electrode array was also evaluated as H_2O_2 may locally be produced during the oxidation of lactate. A cross-talking is often observed from the emission of the hydrogen peroxide from one sensor and its detection by the other sensor [50].

Calibration curves for both biosensors (lactate and glucose) were performed at a fixed potential (E_{app}= +0.15 V vs. SCE) in the presence of 2 mM H_2O_2. No cross-talking signal was observed (Figures 2A and B SM, black curves), thus attesting that the Au microneedle/Au-MWCNTs/pMB modified biosensors were H_2O_2 insensitive.

Formatted: Font color: Background 1

3.3 Effect of pH, Temperature and Interferences on the Biosensor Arrays

The effects of pH and temperature on the proposed lactate and glucose biosensor arrays were evaluated and the results are shown in Figures 4A and B, respectively (LOX = black line and FADGDH = red line). pH influence was studied by varying the pH of the artificial ISF in the range from 5 to 9 by using acetate, MOPS, phosphate and TRIS buffers. For the lactate biosensor the current signal increased with pH until pH 6.5, while in case of the glucose biosensor the optimum pH was found to be 7, values both close to human physiological conditions. The optimum temperature resulted to be 35 °C in both cases (Fig. 4B). pH and temperature results suggested that the microneedle-based biosensor arrays can be successfully used in human physiological conditions both in rest conditions and

during exercise, when body temperature is increasing.

The selectivity of the proposed electrode array was also studied to evaluate the effect of possible interfering compounds on its response. The signals obtained for fixed concentrations of lactate and glucose were compared to those obtained with same concentrations of different interfering compounds such as ascorbic acid, uric acid and glucose or lactate, respectively (LOX = black bars and FADGDH = red bars). No significant currents were observed (Fig. 4D), attesting a very highselectivity of the proposed second generation biosensors thanks to their low operating potential,, due to the combined use of the nanostructuration and the electropolymerization of the mediator MB [46].

3.4 Evaluation of the Biosensor Array Stability and Lifetime

The storage stability of the proposed electrode arrays was investigated by monitoring the current decrease when the electrode arrays are used for 20 measurements every day over a period of 30 days in continuous presence of 0.2 mM glucose (red curve) and 0.2 mM lactate (black curve), respectively, in ISF at pH 7, as reported in Fig. 4C. In particular, LOX based biosensor showed a signal decrease of its initial response of less than 20% after 30 days, probably due to a combination of the intrinsic stability of the enzyme, the nanostructuring of the microneedle electrode surface and to the particular geometry of the microneedles themselves. FADGDH based microneedle electrode showed a signal loss of about 12% after 5 days but a final retained activity of 82% after 30 days, similar to the LOX based biosensor. The lower performance in terms of stability of FADGDH based platform in the first 5 days can be ascribed to the fact that glucose is always present in the ISF unlike lactate. Therefore FADGDH based electrode is always under turnover conditions thus achieving a saturation condition earlier than the LOX based platform.

3.5 Simultaneous Monitoring of Lactate and Glucose in Artificial ISF

The proposed microneedle-biosensor array was tested in flow conditions by using as electrochemical cell a chitosan/agarose hydrogel in order to reproduce a skin model [51-52]. This system allowed to investigate the influence of substrates diffusion in the hydrogel network, which is really close to dermis. The hydrogel was embedded in artificial ISF containing 12 mM lactate and 10 mM glucose, in order to simulate the lactate and glucose concentrations generated after 100 minutes of cycling exercise and after a meal for a healthy patient [53], respectively.

Figure 5 shows the chronoamperograms obtained after injecting 12 mM L-lactate and 10 mM glucose.

The response time resulted to be slower compared to experiments performed in solution, namely 120 seconds for both electrode platforms, probably due to the substrate diffusion through the hydrogel. After 110 hours of continuous measurements, the signals resulted to be really stable unequivocally proving the robustness of the developed microneedles-biosensor array.

Table 1 shows a comparison of the results obtained with other simultaneous amperometric glucose and lactate biosensor arrays reported in literature. Both analytes were detected in different biological fluids such as sweat and horse serum. The linear ranges reported are generally broader but the sensitivities obtained are definitely lower than that obtained with the microneedles-based biosensor array [54-56]. Moreover, the composition of sweat is more variable compared to the composition of the interstitial fluid, being affected by several external factors, such as the presence of microbes on the skin, and it is not always easily collected, for example most of the times it is necessary to stimulate sweating. For these reasons, the interstitial fluid, being a more accessible and reproducible matrix, can be definitely considered the most suitable human body fluid for the minimally invasive detection of L-lactate and glucose.

4. Conclusions

In this study the first example of a second generation minimally invasive biosensor for simultaneous detection of lactate and glucose based on microneedle arrays is proposed The new biosensor device consists of a gold microneedles electrode modified with MWCNTs, polymethylene blue and two enzymes: lactate oxidase from *Aereococcus viridans* on the first working electrode and FAD-glucose dehydrogenase from *Aspergillus niger* on the second electrode. The biosensor array displays highly sensitivity, selectivity and stability for the determination of lactate and glucose in human interstitial fluid. It resulted also inherently not sensitive to the concentration of hydrogen peroxide. The analytical characteristics of the biosensor array are better than those obtained with other biosensors operating in different fluids, such as serum and sweat. Finally, the system was also successfully tested in flow conditions by using as electrochemical cell a chitosan/agarose hydrogel in order to reproduce a skin model.

We can conclude that all these characteristics make this device a promising example of wearable biosensor which can be used in sport medicine and in clinical care for the continuous monitoring of lactate and glucose. Further studies will be carried out to optimize and validate the proposed device for *in vivo* measurements in healthy volunteers and future efforts will focus on the integration of the

instrumentation for signal processing and wireless communication, as well as on the critical evaluation of the tolerability and biocompatibility of the system.

5. Acknowlegments

The authors would like to acknowledge the Italian Research Council for financial support.

6. References

[1] S. Giannos, *Journal of Drug Delivery Science and Technology* **2014**, *24*, 293-299.
[2] G. W. Cleary, Springer, **2011**.
[3] M. R. Prausnitz, H. S. Gill, J.-H. Park, *Modified release drug delivery. Informa Healthcare, New York* **2008**.
[4] M. R. Prausnitz, M. G. Allen, I.-J. Gujral, Google Patents, **2008**.
[5] M. R. Prausnitz, *Advanced drug delivery reviews* **2004**, *56*, 581-587.
[6] P. M. Wang, M. Cornwell, M. R. Prausnitz, *Diabetes technology & therapeutics* **2005**, *7*, 131-141.
[7] Y. Yoon, G. S. Lee, K. Yoo, J.-B. Lee, *Sensors* **2013**, *13*, 16672-16681.
[8] P. R. Miller, S. A. Skoog, T. L. Edwards, D. M. Lopez, D. R. Wheeler, D. C. Arango, X. Xiao, S. M. Brozik, J. Wang, R. Polsky, *Talanta* **2012**, *88*, 739-742.
[9] L. Yu, F. Tay, D. Guo, L. Xu, K. Yap, *Sensors and Actuators A: Physical* **2009**, *151*, 17-22.
[10] C. L. Byers, J. H. Schulman, D. I. Whitmoyer, Google Patents, **1989**.
[11] V. Gartstein, D. D. Nebrigic, G. D. Owens, F. F. Sherman, V. V. Yuzhakov, Google Patents, **2002**.
[12] A. El-Laboudi, N. S. Oliver, A. Cass, D. Johnston, *Diabetes technology & therapeutics* **2013**, *15*, 101-115.
[13] S. Henry, D. V. McAllister, M. G. Allen, M. R. Prausnitz, *Journal of pharmaceutical sciences* **1998**, *87*, 922-925.
[14] S. Byun, J.-M. Lim, S.-J. Paik, A. Lee, K.-i. Koo, S. Park, J. Park, B.-D. Choi, J. M. Seo, K.-a. Kim, *Journal of Micromechanics and Microengineering* **2005**, *15*, 1279.
[15] M. A. Kosoglu, R. L. Hood, Y. Chen, Y. Xu, M. N. Rylander, C. G. Rylander, *Journal of biomechanical engineering* **2010**, *132*, 091014.
[16] C. O'Mahony, F. Pini, A. Blake, C. Webster, J. O'Brien, K. G. McCarthy, *Sensors and Actuators A: Physical* **2012**, *186*, 130-136.
[17] A. Gruetzmann, S. Hansen, J. Müller, *Physiological measurement* **2007**, *28*, 1375.
[18] L.-S. Hsu, S.-W. Tung, C.-H. Kuo, Y.-J. Yang, *Sensors* **2014**, *14*, 12370-12386.
[19] S. Sharma, Z. Huang, M. Rogers, M. Boutelle, A. E. Cass, *Analytical and bioanalytical chemistry* **2016**, *408*, 8427-8435.
[20] P. Bollella, S. Sharma, A. E. G. Cass, R. Antiochia, *Biosensors and Bioelectronics* **2018**.
[21] M. F. Milosevic, A. W. Fyles, R. P. Hill, *International Journal of Radiation Oncology* Biology* Physics* **1999**, *43*, 1111-1123.
[22] J. P. Bantle, W. Thomas, *The Journal of laboratory and clinical medicine* **1997**, *130*, 436-441.
[23] M. Milosevic, A. Fyles, D. Hedley, M. Pintilie, W. Levin, L. Manchul, R. Hill, *Cancer research* **2001**, *61*, 6400-6405.
[24] E. Mukerjee, S. Collins, R. Isseroff, R. Smith, *Sensors and Actuators A: Physical* **2004**, *114*, 267-275.
[25] T. M. Rawson, S. Sharma, P. Georgiou, A. Holmes, A. Cass, D. O'Hare, *Electrochemistry Communications* **2017**, *82*, 1-5.
[26] T. Rawson, S. Gowers, M. Rogers, E. Sallabank, S. Sharma, P. Georgiou, A. Holmes, T. Cass, D. O'Hare, *International Journal of Infectious Diseases* **2018**, *73*, 109.
[27] S. Paliwal, B. H. Hwang, K. Y. Tsai, S. Mitragotri, *European journal of pharmaceutical sciences* **2013**, *50*, 546-556.
[28] J. R. Windmiller, N. Zhou, M.-C. Chuang, G. Valdés-Ramírez, P. Santhosh, P. R. Miller, R. Narayan, J. Wang, *Analyst* **2011**, *136*, 1846-1851.

[29] P. R. Miller, R. J. Narayan, R. Polsky, *Journal of Materials Chemistry B* **2016**, *4*, 1379-1383.
[30] G. Valdés-Ramírez, Y.-C. Li, J. Kim, W. Jia, A. J. Bandodkar, R. Nuñez-Flores, P. R. Miller, S.-Y. Wu, R. Narayan, J. R. Windmiller, *Electrochemistry Communications* **2014**, *47*, 58-62.
[31] L. Ventrelli, L. Marsilio Strambini, G. Barillaro, *Advanced healthcare materials* **2015**, *4*, 2606-2640.
[32] S. Sharma, A. Saeed, C. Johnson, N. Gadegaard, A. E. Cass, *Sensing and Bio-Sensing Research* **2017**, *13*, 104-108.
[33] A. V. Mohan, J. R. Windmiller, R. K. Mishra, J. Wang, *Biosensors and Bioelectronics* **2017**, *91*, 574-579.
[34] Y. Umena, K. Yorita, T. Matsuoka, A. Kita, K. Fukui, Y. Morimoto, *Biochemical and biophysical research communications* **2006**, *350*, 249-256.
[35] S. Tsujimura, S. Kojima, K. Kano, T. Ikeda, M. Sato, H. Sanada, H. Omura, *Bioscience, biotechnology, and biochemistry* **2006**, *70*, 654-659.
[36] N. Fogh-Andersen, B. M. Altura, B. T. Altura, O. Siggaard-Andersen, *Clinical chemistry* **1995**, *41*, 1522-1525.
[37] A. E. Cass, S. Sharma, in *Methods in enzymology, Vol. 589*, Elsevier, **2017**, pp. 413-427.
[38] X. Dai, R. G. Compton, *Electroanalysis: An International Journal Devoted to Fundamental and Practical Aspects of Electroanalysis* **2005**, *17*, 1325-1330.
[39] A. Silber, N. Hampp, W. Schuhmann, *Biosensors and Bioelectronics* **1996**, *11*, 215-223.
[40] A. Karyakin, A. Strakhova, E. Karyakina, S. Varfolomeyev, A. Yatslmirsky, *Synthetic metals* **1993**, *60*, 289-292.
[41] A. A. Karyakin, E. E. Karyakina, H. L. Schmidt, *Electroanalysis: An International Journal Devoted to Fundamental and Practical Aspects of Electroanalysis* **1999**, *11*, 149-155.
[42] V. Zamora-Mora, D. Velasco, R. Hernández, C. Mijangos, E. Kumacheva, *Carbohydrate Polymers* **2014**, *111*, 348-355.
[43] P. Babij, S. Matthews, M. Rennie, *European journal of applied physiology and occupational physiology* **1983**, *50*, 405-411.
[44] D. H. Elwyn, J. M. Kinney, M. Jeevanandam, F. E. Gump, J. R. Broell, *Annals of Surgery* **1979**, *190*, 117.
[45] G. Jobst, I. Moser, M. Varahram, P. Svasek, E. Aschauer, Z. Trajanoski, P. Wach, P. Kotanko, F. Skrabal, G. Urban, *Analytical Chemistry* **1996**, *68*, 3173-3179.
[46] F. W. Campbell, S. R. Belding, R. G. Compton, *ChemPhysChem* **2010**, *11*, 2820-2824.
[47] D. Menshykau, I. Streeter, R. G. Compton, *The Journal of Physical Chemistry C* **2008**, *112*, 14428-14438.
[48] J. Kulys, L. Wang, A. Maksimoviene, *Analytica chimica acta* **1993**, *274*, 53-58.
[49] M. N. Zafar, N. Beden, D. Leech, C. Sygmund, R. Ludwig, L. Gorton, *Analytical and bioanalytical chemistry* **2012**, *402*, 2069-2077.
[50] F. Palmisano, R. Rizzi, D. Centonze, P. Zambonin, *Biosensors and Bioelectronics* **2000**, *15*, 531-539.
[51] S. P. Miguel, M. P. Ribeiro, H. Brancal, P. Coutinho, I. J. Correia, *Carbohydrate polymers* **2014**, *111*, 366-373.
[52] B. V. Slaughter, S. S. Khurshid, O. Z. Fisher, A. Khademhosseini, N. A. Peppas, *Advanced materials* **2009**, *21*, 3307-3329.
[53] O. Schweizer, W. S. Howland, C. Sullivan, E. Vertes, *Anesthesiology* **1967**, *28*, 814-822.
[54] A. F. Revzin, K. Sirkar, A. Simonian, M. V. Pishko, *Sensors and Actuators B: Chemical* **2002**, *81*, 359-368.

[55] W. Gao, S. Emaminejad, H. Y. Y. Nyein, S. Challa, K. Chen, A. Peck, H. M. Fahad, H. Ota, H. Shiraki, D. Kiriya, *Nature* **2016**, *529*, 509.
[56] P. Petrou, I. Moser, G. Jobst, *Biosensors and Bioelectronics* **2003**, *18*, 613-619.

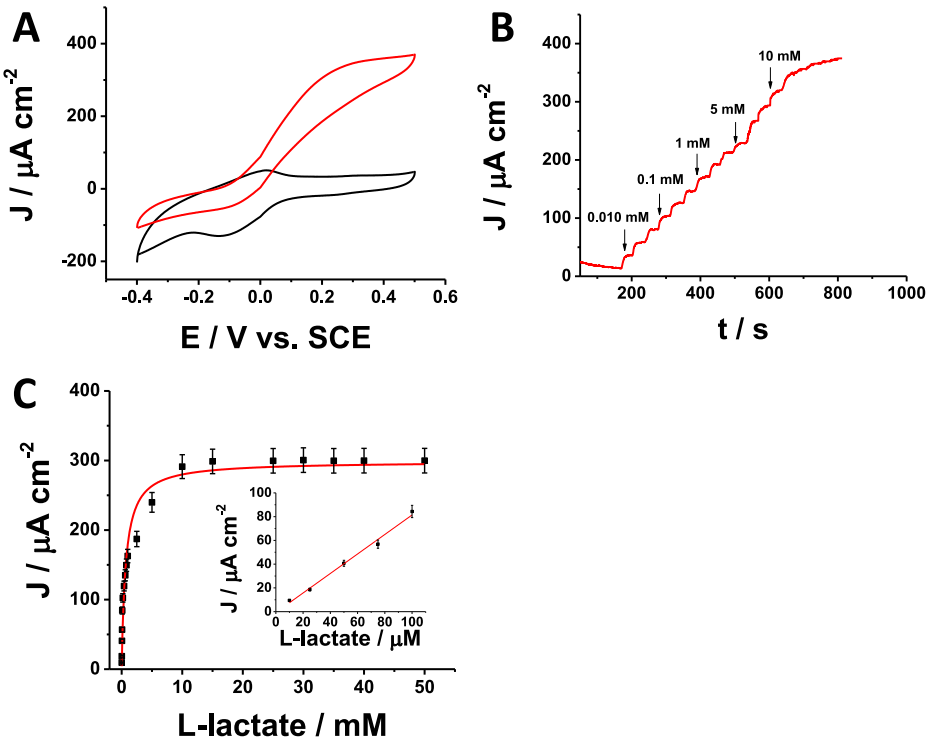

Fig. 2. (A) CVs of Au microneedle/Au-MWCNTs/pMB/LOX in absence (black) and in presence (red) of 10 mM L-lactate. Experimental conditions: artificial ISF at pH 7; scan rate 5 mV s^{-1} and T= 25 °C; (B) Chronoamperogram performed with Au microneedles/Au-MWCNTs/pMB/LOX in artificial ISF. Experimental conditions: substrate L-lactate, applied potential + 0.15 V vs. SCE, adding time = 40 s, under stirring = 400 rpm and T = 25 °C; (C) Calibration curve performed with Au microneedles/Au-MWCNTs/pMB/LOX in artificial ISF. Experimental conditions: substrate L-lactate, applied potential + 0.15 V vs. SCE, adding time = 40 s, under stirring = 400 rpm and T = 25 °C. Inset: low micromolar range.

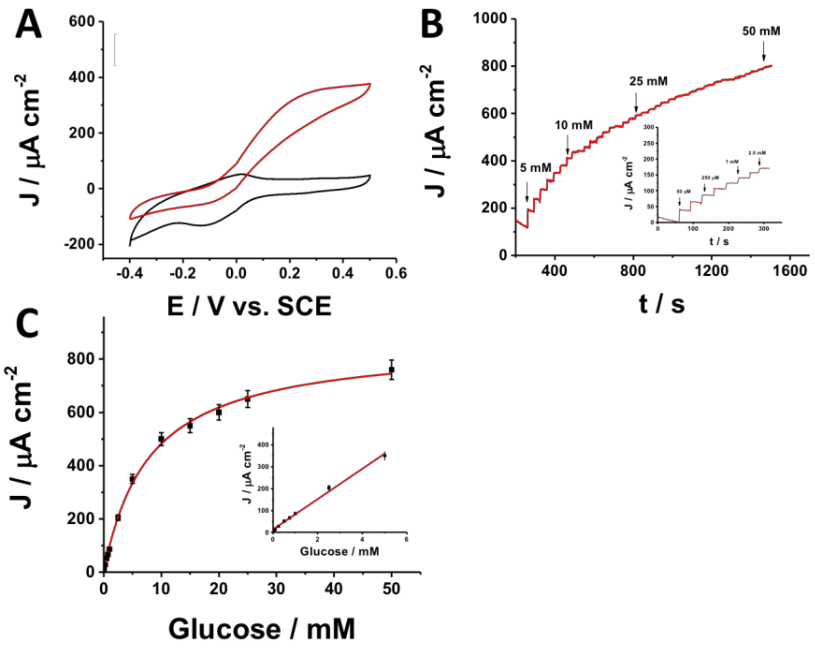

Fig. 3. (A) CVs of Au microneedle/Au-MWCNTs/pMB/FADGDH in absence (black) and in presence (red) of 10 mM glucose. Experimental conditions: artificial ISF at pH 7; scan rate 5 mV s^{-1} and T= 25 °C; **(B)** Chronoamperogram performed with Au microneedles/Au-MWCNTs/pMB/FADGDH in artificial ISF. Experimental conditions: substrate glucose, applied potential + 0.15 V vs. SCE, adding time = 40 s, under stirring = 400 rpm and T = 25 °C. Inset: low micromolar range; **(C)** Calibration curve performed with Au microneedles/Au-MWCNTs/pMB/FADGDH in artificial ISF. Experimental conditions: substrate glucose, applied potential + 0.15 V vs. SCE, adding time = 40 s, under stirring = 400 rpm and T = 25 °C. Inset: low micromolar range.

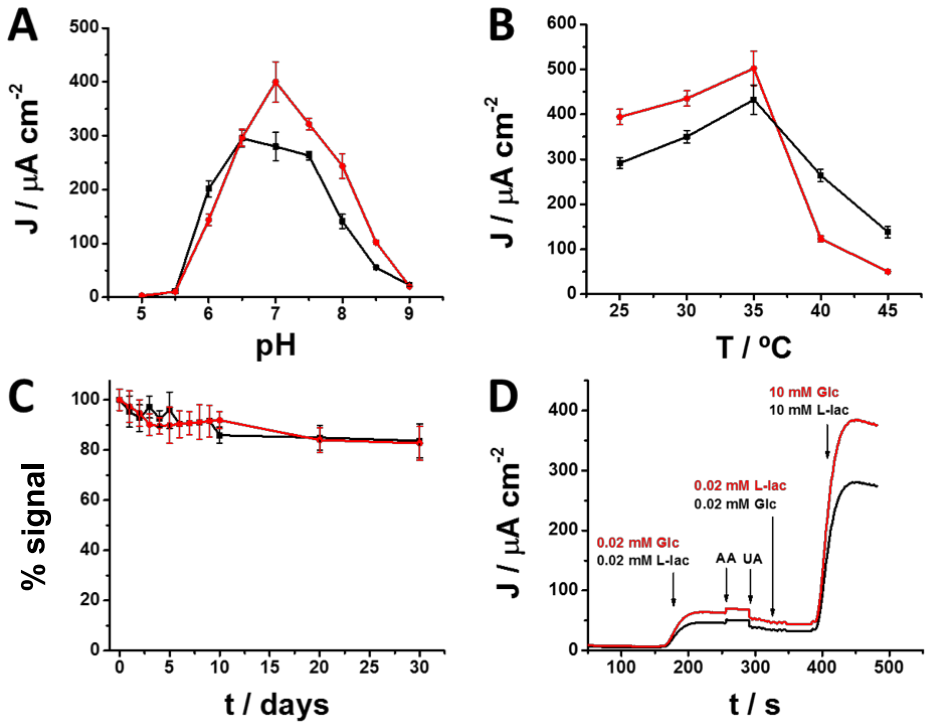

Fig. 4. (A) Effect of different pH on Au microneedle/Au-MWCNTs/pMB/LOX (black line) and Au microneedle/Au-MWCNTs/pMB/FADGDH (red line) based biosensor array. Experimental conditions: artificial ISF at different pHs (5-9), 10 mM L-lactate and 10 mM Glucose, applied potential + 0.15 V, T = 25 °C. (B) Effect of different temperatures on Au microneedle/Au-MWCNTs/pMB/LOX (black line) and Au microneedle/Au-MWCNTs/pMB/FADGDH (red line) based biosensor array. Experimental conditions: artificial ISF at pH 7, 10 mM L-lactate and 10 mM Glucose, applied potential + 0.15 V. (C) Stability measurements carried out over a period of 30 days for Au microneedle/Au-MWCNTs/pMB/LOX (black line) and Au microneedle/Au-MWCNTs/pMB/FADGDH (red line) based biosensor array in presence of 0.2 mM L-lactate and 0.2 mM glucose in artificial ISF at pH 7; E_{app} = 0.150 vs. SCE; T = 25 ° C. (D) Influence of interfering compounds on lactate response (black line): 20 µM L-lactate (L-lac), 20 µM ascorbic acid (AA), 20 µM uric acid (UA), 20 µM glucose (Glc) and 10 mM L-lactate. Influence of interfering compounds on glucose response (red line): 20 µM glucose (Glc), 20 µM ascorbic acid (AA), 20 µM uric acid (UA), 20 µM L-lactate (L-lac) and 10 mM glucose (Glc). Experimental conditions: artificial ISF, applied potential + 0.15 V vs. SCE, adding time = 40 s, under stirring = 400 rpm and T = 25 °C.

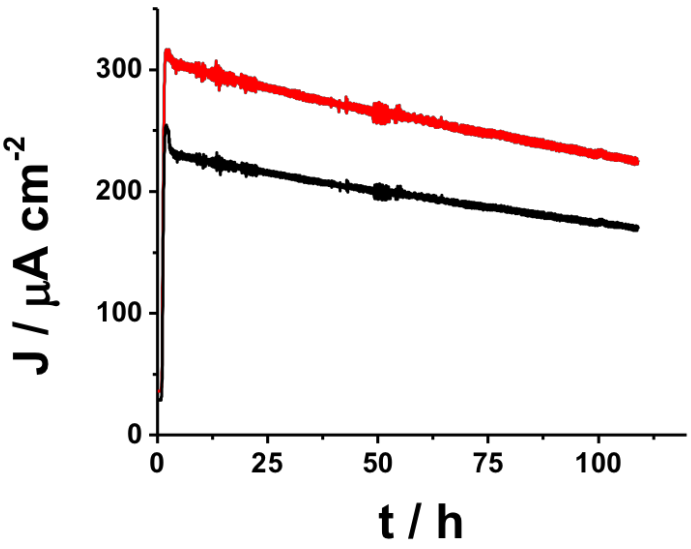

Fig 5. Chronoamperograms performed with Au microneedles/Au-MWCNTs/pMB/LOX (black line) and Au microneedles/Au-MWCNTs/pMB/FADGDH (red line) in chitosan/agarose hydrogel embedded in artificial ISF. Experimental conditions: substrate 10 mM glucose and 12 mM L-lactate, applied potential + 0.15 V vs. SCE, T = 25 °C.

Table 1. Comparison with other biosensor arrays for lactate and glucose detection reported in literature.
List of abbreviations in alphabetic order: 11-mercaptoundecanoic acid (MUA), chitosan (chit), glucose oxidase (GOX), gold electrode (AuE), gold-multiwalled carbon nanotubes electrodeposited (Au-MWCNTs), interstitial fluid (ISF), L-lactate oxidase (LOX), multi-walled carbon nanotubes (MWCNTs), platinum electrode (PtE), poly-2-hydroxyethyl methacrylate (polyHEMA), poly[vinylpyridine Os(bis-bipyridine)$_2$Cl]-co-allylamine (PVP-Os-AA), polymethylene blue (pMB), prussian blue (PB).

Electrode Platform	Sensing Fluids	Sensor Type	Linear Range (mM)	Sensitivity	Generation	Reference
GOX/Chit /MWCNTs/PB/AuE **LOX/Chit /MWCNTs/PB/AuE**	Sweat	Bendable	0 – 0.2 2 – 30	2.35 nA μM^{-1} 220 nA mM^{-1}	1st generation	[55]
GOX/PolyHEMA/PtE **LOX/PolyHEMA/PtE**	Horse serum	Solid electrode on glass support	0 – 15 0 – 30	0.27 nA mM^{-1} 0.36 nA mM^{-1}	1st generation	[56]
GOX/PVP-Os-AA/MUA/AuE **LOX/PVP-Os-AA/MUA/AuE**	-	Patterned solid electrode on glass support	0 – 20 0 – 10	0.26 $\mu A\ cm^{-2}\ mM^{-1}$ 0.24 $\mu A\ cm^{-2}\ mM^{-1}$	2nd generation	[54]
GDH/pMB/Au-MWCNTs/AuE **LOX/pMB/Au-MWCNTs/AuE**	ISF	Microneedles	0.05 – 5 0.01 – 0.1	405.2 $\mu A\ cm^{-2}\ mM^{-1}$ 797.4 $\mu A\ cm^{-2}\ mM^{-1}$	2nd generation	This work

Supporting Material

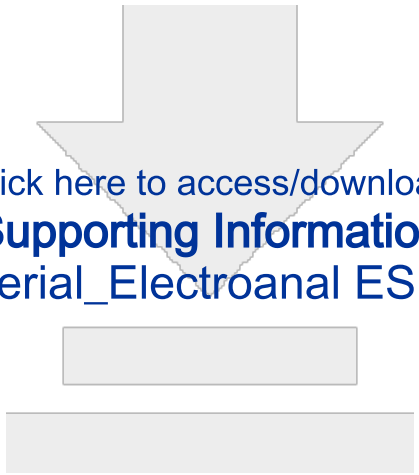

Click here to access/download

Supporting Information

Supporting material_Electroanal ESEAC 2018.docx

Cover letter